Latex Film Formation in the Presence of Organic Solvents

Didier Juhué and Jacques Lang*

Institut Charles Sadron (CRM-EAHP), CNRS-ULP Strasbourg, 6 rue Boussingault, 67083 Strasbourg Cedex, France

Received June 25, 1993; Revised Manuscript Received September 15, 1993®

ABSTRACT: The effect of five organic solvents on polymer diffusion across particle interfaces in poly(butyl methacrylate) latex films annealed above their glass-transition temperature has been studied by fluorescent nonradiative energy transfer. Diffusion coefficients and penetration depths of polymer chains were calculated by assuming a Fickian diffusion. Their variations upon annealing time were found to depend on the nature of the organic solvent. A qualitative model describing the variation of penetration depth with time, accounting for solvent plasticizing effect and evaporation, is presented.

Introduction

Many studies have been carried out on latex film formation because of its great importance in paint, coating, paper, and adhesive industries. They led to the general conclusion that film formation occurs in three main steps: (i) a linear cumulative water loss with time, the evaporation rate of which was close to the one of pure water (this step ends when irreversible contact between particles is achieved (particle volume fraction between 60 and 74%)); (ii) particle deformation and close contact associated with a dramatic decrease of the water evaporation rate (this leads to a dry film presenting the so-called honeycomb structure where particle contours are still visible); (iii) polymer interdiffusion across particle boundaries, known as further gradual coalescence[1] or autohesion,[2] yielding a homogeneous film.

Several studies showed that the extent of this third step determines the goodness of mechanical properties of the films. One way to promote polymer diffusion across particle boundaries is to add to latex dispersions small quantities of organic solvent, called on purpose coalescing aids. Their action mode is understood as a temporary plasticization which favors polymer chain motions. However the solvent is expected to evaporate off the film in order to retrieve the mechanical properties of the additive-free film.

In this paper we show the effect of five organic solvents on polymer interdiffusion across particle boundaries, followed using the fluorescent nonradiative energy transfer technique first developed by Winnik and his co-workers,[3-5] in poly(butyl methacrylate) (PBMA) latex films. The effect of coalescing aids on latex film formation has already been investigated with this technique.[6-8] As in these previous works the data analysis was done in terms of Fickian diffusion of the latex polymer chains. In our study we calculated the interpenetration distances of the polymer chains and related them to the organic solvent evaporation rates and partition coefficients between water and polymer phases. Finally, in the present study the term filming aid is preferred to coalescing aid because our experiments deal with large interpenetration distances.

Materials and Methods

Materials. Sodium dodecyl sulfate (Touzard et Matignon) was recrystallized thrice from mixtures of water and ethanol. Potassium persulfate and butyl methacrylate (BMA) were purchased from Aldrich (99%), and sodium hydrogen carbonate from Prolabo (RP Normapur). (9-Phenanthryl)methyl methacrylate (PheMMA) and 9-Anthryl methacrylate (AnMA) were kindly synthesized by Dr. Fouqué (Elf Atochem, CAL) following the recipe given elsewhere.[4] Water was freshly deionized and distilled before use. Organic solvents, diethylene glycol monobutyl ether (DGB) (Fluka >98% GC), diacetone alcohol (DA) (Fluka ~99% GC), 2,2,4-trimethyl-1,3-pentanediol monoisobutyrate (TPM) (Eastman Kodak), and hexylene glycol (HG) and benzyl alcohol (ABY) (Merck spectrograde), were used as received.

Latex Synthesis. Labeled latex particles were synthesized by free radical emulsion polymerization following the procedure described by Zhao et al.[4] It is a semicontinuous reaction where the fluorescent monomer (about 1 monomer mol % PheMMA or AnMA) dissolved in BMA is slowly added (50 μL/min, starving conditions) into the reactor to the seed (12 wt % of the total BMA) in the second stage. With this procedure one can assure a good repartition of the fluorescent dyes in the latex particles. Molecular weights (M_w = 600 000 and M_n = 80 000 for P(PheMMA-BMA) and M_w = 500 000 and M_n = 44 000 for P(AnMA-BMA)) were calculated according PMMA standards using gel permeation chromatography (GPC). These molecular weights of 600 000 and 500 000 correspond to a gyration radius of PBMA chains of 16.5 and 15 nm, respectively.[9]

Particle diameters were determined by quasi-elastic light scattering and found to be equal to 140 nm. Particles are monodisperse in size, as observed as a part of this work by atomic force microscopy (variation in diameter less than 10 nm). Latex dispersions have a 26% solid content. Proper labeling of the polymer chains was checked using a UV detector coupled to the GPC apparatus. The presence of absorption peaks at 298 and 355 nm, for phenanthrene and anthracene, respectively, at the same elution time as that of the mass peaks and the absence of absorption peak at the low molecular weight elution times assured a complete reaction of the fluorescent monomers.

Latex Dispersion Preparation. Latex dispersions were prepared by adding weighed amounts of organic solvents (10 wt % based on polymer) to a 1:1 mixture of P(PheMMA-BMA) and P(AnMA-BMA) latices. Those dispersions were allowed to equilibrate under gentle stirring for 8 days.

Latex Film Preparation. Latex films were prepared by casting 2–3 drops of dispersion onto quartz plates (ca. 20 mm × 10 mm) and allowed to air dry at 17 °C for 1.5 h. Dry films were about 100 μm thick. Films were also kept under an argon atmosphere during annealing and storage (8 °C) times.

Fluorescence Decay Measurements. Donor (phenanthrene) fluorescence decay traces were measured with a single photon counting apparatus.[10] Film samples, mounted on a homemade solid sample holder were excited at 298 nm, and the emission light was collected through a band-pass filter (Schott) centered at 366 nm to minimize the uptake of scattered and acceptor (anthracene) emitted light. All measurements were performed at 10 °C (~26 deg below T_g) to avoid any kind of evolution of films during the illumination time.

The analysis of the fluorescence decay profile was done as described by Winnik et al.[4,5] The model, derived from the Förster theory,[11] of nonradiative energy transfer is based on the fact that

® Abstract published in *Advance ACS Abstracts*, January 1, 1994.

0024-9297/94/2227-0695$04.50/0

donor and acceptor pairs are randomly distributed in the film and are static during the fluorescence measurements. The efficiency of energy transfer depends only on the average donor–acceptor distance in a range of 0–50 Å. Thus the donor fluorescence decay $I_D(t)$ can be expressed by the sum of two contributions weighted by the preexponential factors B_1 and B_2, on the one hand from the donors in the mixed domains, and from the donors in the not yet mixed domains on the other hand, respectively:

$$I_D(t) = B_1 \exp(-t/\tau_D - p(t/\tau_D)^{1/2}) + B_2 \exp(-t/\tau_D) \quad (1)$$

where p is a time-independent parameter proportional to the local concentration of acceptors and τ_D is the donor fluorescence lifetime that was found equal to 46 ns in a P(PheMMA–BMA) latex film. The parameters B_1, B_2, and p are obtained by fitting eq 1 to the donor fluorescence decay data using a nonlinear weighted least-squares procedure. An apparent volume fraction of mixing $f'_m(t)$ can be defined as the ratio B_1 over $B_1 + B_2$. This fraction has to be corrected for energy transfer taking place at particle boundaries in nascent films and replaced by a normalized volume fraction of mixing $f_m(t)$ in eq 2. $f'_m(\infty)$ corresponds to a

$$f_m(t) = \frac{f'_m(t) - f'_m(0)}{f'_m(\infty) - f'_m(0)} \quad (2)$$

fully mixed film and was obtained from a latex film dissolved in THF and solution-cast onto a quartz plate. A value of 0.97 was found, which is a satisfactory value. The average value of $f'_m(0)$ for all nascent films formed at 17 °C was 0.16, which is quite reasonable since it corresponds to a shell 40 Å thick. However, as mentioned by Juhué et al.,[8] the postaddition of coalescing aids makes $f'_m(0)$ larger, e.g., from 0.18 to 0.23. This certainly means that polymer interdiffusion across particle boundaries occurs as soon as particles are in close contact, because of the lowering of the glass-transition temperature of the latex polymer. Note that another role of the solvent is to lower the elastic modulus of the particles, promoting their deformation and the wetting process.[12]

Data Treatment. In order to give a physical quantification of the polymer diffusion, one has to relate f_m measurements to physical parameters such as diffusion coefficients D. This was done in previous works.[4,5] When a spherical Fickian model of diffusion was assumed a concentration profile $c(r,t)$ of the donor polymer chains corresponding to a diffusion coefficient D could be calculated. The D value was then optimized in order to match an experimental f_m value to its theoretical expression:

$$f_m(t) = 1 - \frac{1}{V_0}\int_0^{R_0} \frac{c(r,t)}{c_0} 4\pi r^2 \, dr \quad (3)$$

where V_0 is the volume of a particle of radius R_0.

An analytical solution of $c(r,t)$ to the differential equation of Fick's law can be derived in the case of no initial diffusion ($f_m(0) = 0$).[13] But in the case of a nonzero $f_m(0)$ value, a numerical method had to be developed through software.[8] In short, this method, known as the finite-difference method,[14] consists of generating a discrete model of $c(r,t)$. The initial $c(r,0)$ corresponding to the non-zero $f_m(0)$ value is calculated and then taken into account to calculate those at greater annealing times. The software operates by successive iterations to optimize D as mentioned above, using a dichotomy method.[15]

In previous studies[4,5] calculated diffusion coefficients $D(t)$ corresponded to the polymer diffusion observed between the annealing times $t = 0$ and t and therefore were cumulative coefficients. In our study we preferred to calculate diffusion coefficients corresponding to the diffusion that occurred between successive annealing times, and thus accessed pseudoinstantaneous coefficients. Although the overall method used here is the same as in previous works[4,5] the pseudoinstantaneous D values are closer to what really happens in the system with annealing.

Another interesting parameter, which quantitatively describes polymer diffusion, is the interpenetration distance or penetration depth of the polymer chains of a latex particle with adjacent particles. In studies on latex film formation done using the small angle neutron scattering technique (SANS),[16–20] a penetration depth d_{R_G} (eq 4) was obtained from the subtraction of the original particle radius R_0 from the radius $R(t)$ of the growing particle:

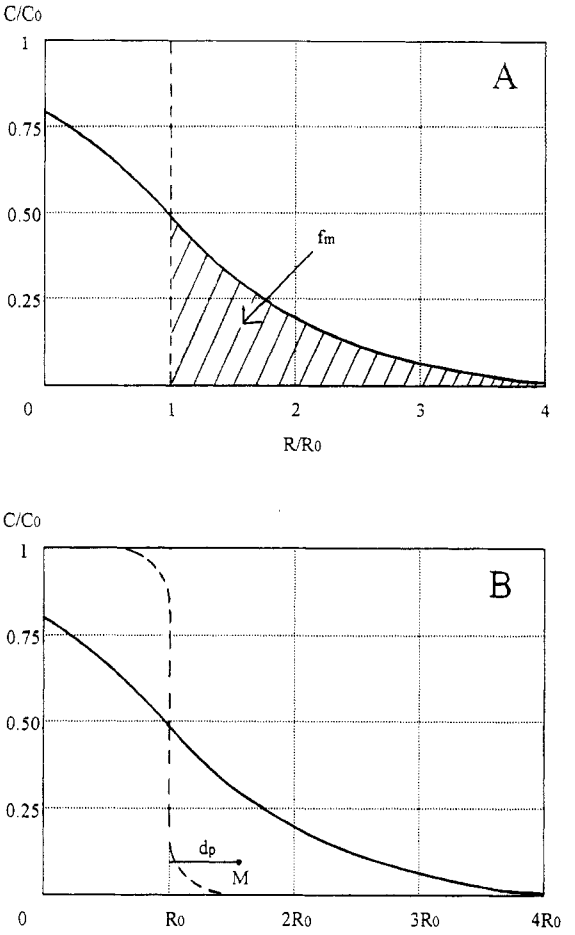

Figure 1. Schematic representation of a donor polymer chain concentration profile: dashed line for the zero (A) and non-zero (B) initial f_m value ($t = 0$); solid line after time t. f_m is the volume fraction of mixing, and d_p, the distance diffused out of the original latex particle.

$$d_{R_G} = R(t) - R_0 \quad (4)$$

with $R(t)$ equal to $(5/3)^{1/2}R_G$, where R_G given in eq 5 is the radius of gyration of a growing particle.

$$R_G^2 = \frac{\int_0^\infty r^2 c(r,t) 4\pi r^2 \, dr}{\int_0^\infty c(r,t) 4\pi r^2 \, dr} \quad (5)$$

Another definition of the penetration depth has been proposed[21] and is given in eq 6.

$$d_p = \frac{\int_{R_0}^\infty r c(r,t) 4\pi r^2 \, dr}{\int_{R_0}^\infty c(r,t) 4\pi r^2 \, dr} - R_0 \quad (6)$$

d_p is therefore the distance traveled by donor labeled polymer chains by diffusion out of their original particle of radius R_0 (see Figure 1). More precisely, d_p represents the distance between R_0 and the center of mass of polymer chains that have diffused out of the original particle.

Finally, we also calculated the displacement d of the mass center of particles for comparison with d_p and d_{R_G}, using eq 7.

$$d = \frac{\int_0^\infty r c(r,t) 4\pi r^2 \, dr}{\int_0^\infty c(r,t) 4\pi r^2 dr} - \frac{3}{4}R_0 \quad (7)$$

Other Measurements. Differential scanning calorimetry measurements (20 °C/min) were carried out using a Perkin-Elmer

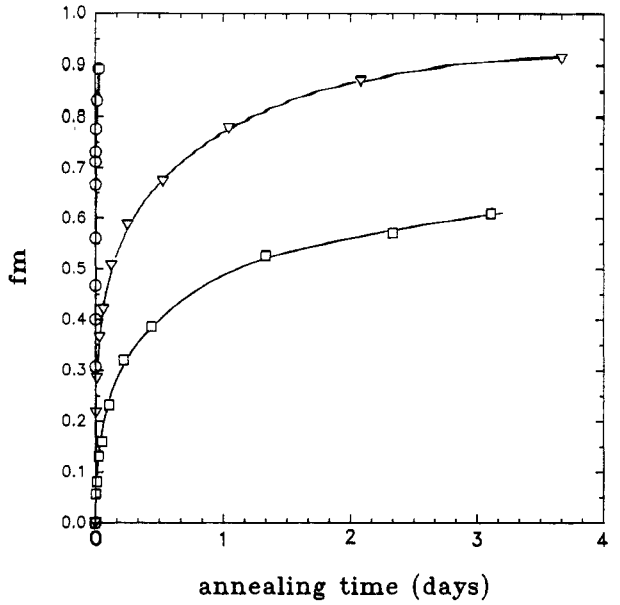

Figure 2. Plots of volume fraction of mixing f_m versus annealing time at 70 °C (□), 90 °C (▽), and 120 °C (○).

DSC7 to determine glass-transition temperatures of latex films with and without organic solvents.

Gas phase chromatography (GPC) was performed using a Hewlett-Packard 5880 (column Porapak P) to obtain partition coefficients K of the organic solvents between the water phase and latex particles. K values were measured by determining the concentration of the organic solvents in the water phase obtained after centrifugation of the latex dispersions.[22]

Thermogravimetric measurements (TGA) were done using a Mettler TA300. A two-step procedure was adopted: films were dried in situ for 2 h at 30 °C to make sure that most of water was evaporated. Then annealing at 70 °C was carried out for 17 h. Mass losses of films versus time were monitored during annealing.

Results and Discussion

1. Volume Fraction of Mixing. Figure 2 shows the plot of f_m versus annealing time for three different films formed at 70, 90, and 120 °C. The drastic effect of the temperature is quite remarkable, especially at short annealing times. At long times the f_m curves converge slowly toward 100% of mixing (not shown). Figure 3 represents the annealing time τ necessary to reach f_m values of 0.25, 0.50, and 0.75 as a function of the temperature. τ values were obtained from the values reported in Figure 2. Thus one can easily get estimate values of τ at 50 °C for instance, i.e. 18 deg above T_g (=36 °C measured by DSC). It would take about 5 days, 2 months, and more than 1 year to reach f_m values of 0.25, 0.50, and 0.75, respectively, compared to 13 s, 1.5 min, and almost 8 mins, respectively, at 120 °C. These remarks again show the tremendous effect of temperature on polymer diffusion.

Figure 4 shows the variations of f_m versus annealing time of films containing the different organic solvents postadded to the latex dispersions, as indicated in the Materials and Methods, and annealed at 70 °C. These plots are represented in two different time scales in order to appreciate the solvent effects at short and long times. After about 7 days of annealing, films containing solvents show f_m values comparable to that of the additive-free latex film (see in Figure 4B). However at short annealing times (see Figure 4A) differences of behavior between additives are much more visible. Three types of behavior can be distinguished: (i) In the case of DA f_m values are rapidly the same as those of an additive-free film. Therefore this solvent may be not a good filming aid if used at this concentration. However its substantial $f_m(0)$ value shows that it could be used as a filming aid at higher concentrations. (ii) ABY, HG, and DGB give rise to a substantial increase of f_m during the first hour of annealing, compared to the solvent-free film. After 2 h f_m levels off and finally slowly converges toward the additive-free film f_m curve. These solvents are therefore efficient at short annealing times and can be considered as rather good filming aids. (iii) TPM shows a totally different behavior from the other solvents. As a matter of fact its efficiency persists long after 1 h of annealing, becoming even larger than the others. Therefore it may be considered rather as an efficient plasticizer than a filming aid. We will see in the following that the different behaviors of the organic solvents are related to their evaporation rates and partition

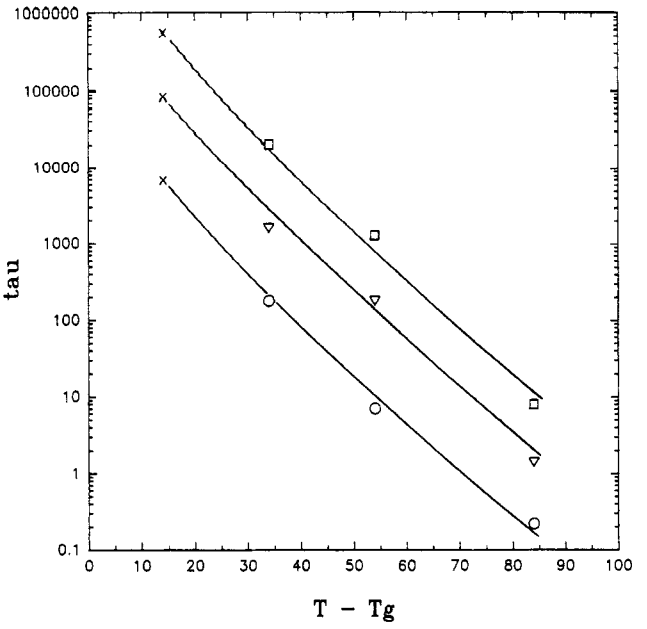

Figure 3. Plots of annealing time τ necessary to reach f_m values of 0.25 (○), 0.50 (▽), and 0.75 (□) against $T - T_g$, where T is the annealing temperature. T_g was taken equal to 36 °C. Crosses represent τ values extrapolated at T = 50 °C.

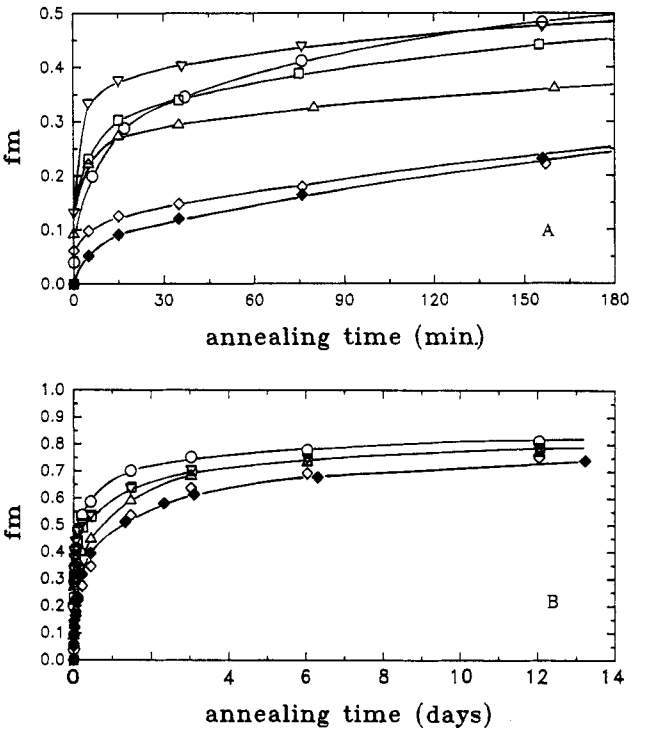

Figure 4. Plots of volume fraction of mixing f_m versus annealing time at 70 °C for films containing DA (◇), ABY (△), HG (□), TPM (○), DGB (▽), and no additive (◆).

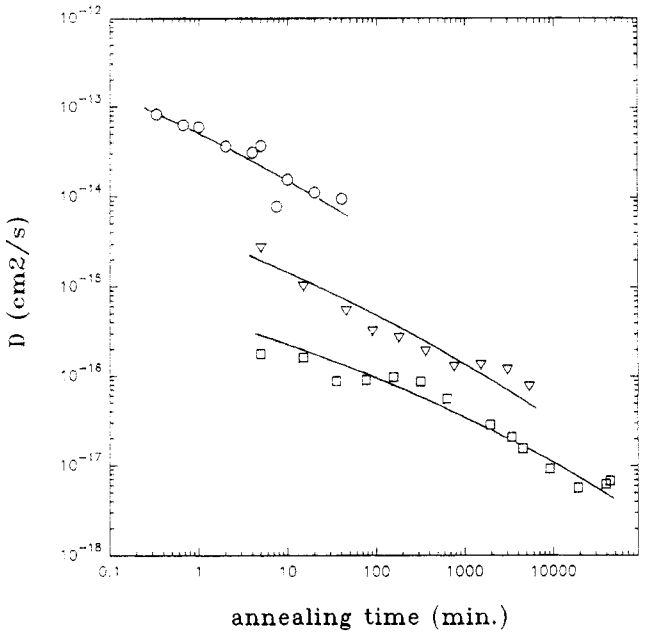

Figure 5. Plots of diffusion coefficients D versus annealing time at 70 °C (□), 90 °C (▽), and 120 °C (○).

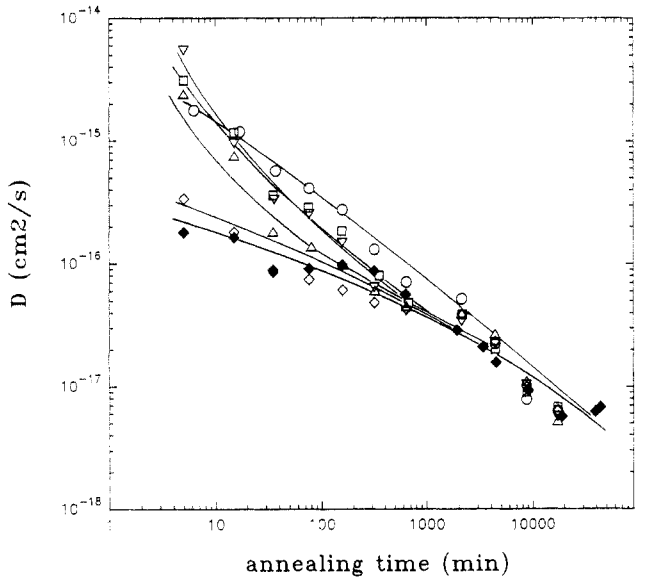

Figure 6. Plots of diffusion coefficients D versus annealing time at 70 °C for films containing DA (◇), ABY (△), HG (□), TPM (○), DGB (▽), and no additive (◆).

coefficients between latex particles and the water phase in the dispersion.[7,22]

2. Diffusion Coefficients. Figure 5 shows plots of diffusion coefficients D versus annealing time for solvent-free films. D values decrease as t increases, whereas they should theoretically be constant since the polymer chain diffusion is independent of its position in the film, except perhaps at particle boundaries at short annealing times where polymer chains may have a constrained conformation. However the decrease in the D values persists even farther than a penetration distance equal to a mean radius of gyration of polymer chains (R_G = 16 nm). Thus it may rather be explained by the large molecular weight polydispersity, as suggested by Hahn et al.[16] in their SANS experiments. As a matter of fact one can easily imagine that diffusion is dominated by short chains at short annealing time and by long chains at long annealing time.

Figure 6 represents variations of diffusion coefficients D versus annealing time at 70 °C for films with and without organic solvents. The presence of organic solvent has a tremendous effect on D values, especially at early annealing times. Notice that D values in films containing solvents are close to the ones in the additive-free film at long annealing times, which indicates a loss of efficiency of organic solvents due to solvent evaporation as time goes by.[7]

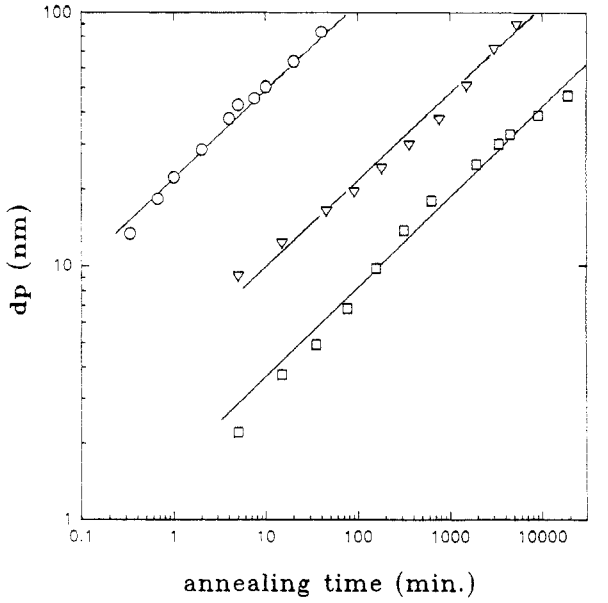

Figure 7. Plots of penetration depth d_p versus annealing time at 70 °C (□), 90 °C (▽), and 120 °C (○).

The D values obtained in our study are of the same order of magnitude as the ones found by others.[4,5,16,17,23]

3. Penetration Depth. Figure 7 shows a log–log representation of the plots of d_p versus time for additive-free films annealed at 70, 90, and 120 °C. Within the accuracy of the fluorescence measurements, these plots are linear and parallel. Here again it is worth stressing the large effect of temperature on d_p. Although d_p may be considered as another representation of f_m, it enables a direct comparison with the particle radius. Thus from Figure 7 the annealing time necessary for the polymer chains to diffuse, for instance, one-tenth of a particle diameter, i.e. about 14 nm, can be estimated to 7 h, 30 min, and 20 s at 70, 90, and 120 °C, respectively. The linearity of the log–log variations of d_p against the annealing time yields a common slope of 0.35 ± 0.10 at the three temperatures. It would mean that d_p varies linearly with $t^{0.35}$ instead of the well-known power law of $t^{0.5}$. There are actually few experimental data in the literature showing evolutions of the penetration depth with time. One example is the study on deuterated polystyrene latex particles using the SANS technique[18–20] where the growth of the radius of gyration of deuterated particles in a matrix of nondeuterated particles was followed with annealing time. The time power law of the penetration depth, in this case d_{R_G} (eq 4), was found equal to 0.49 for polystyrene chains of moderate molecular weight (M_W = 250 000) and 0.38 for high molecular weight polystyrene chains (M_W = 2 000 000). We calculated penetration depths d_{R_G} with the SANS experimental data obtained by Hahn et al.[16] The time power law is 0.58 for PBMA particles of M_w equal to 500 000 annealed at 90 °C. In our experiments log–log variations of d_{R_G} versus time at 70, 90, and 120 °C exhibit an average slope of 0.53 ± 0.10, which is close to what we calculated with the data of Hahn et al. for the same polymer within the accuracy of the measurements.

Figure 8 shows log–log representations of d_p, d, and d_{R_G} versus annealing time at 70 °C in our PBMA latex films. d_{R_G} and d have similar slopes on a logarithmic scale which

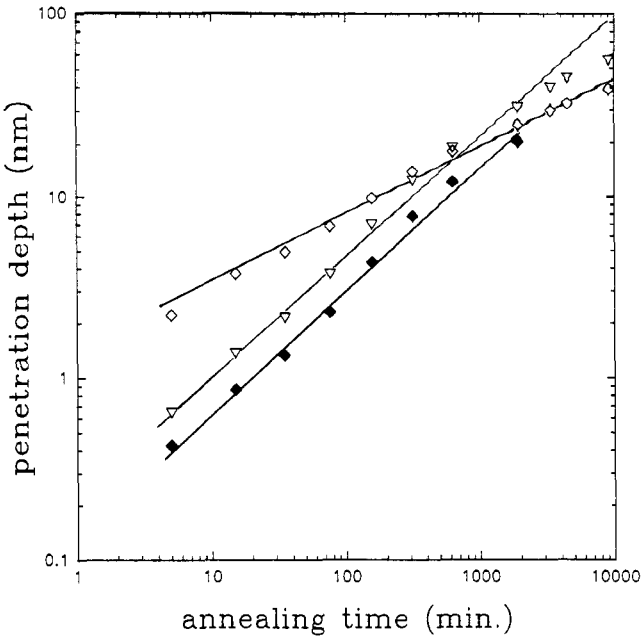

Figure 8. Plots of diffusion distances d_p (◇), d (◆), and d_{R_G} (▽) versus annealing time at 70 °C.

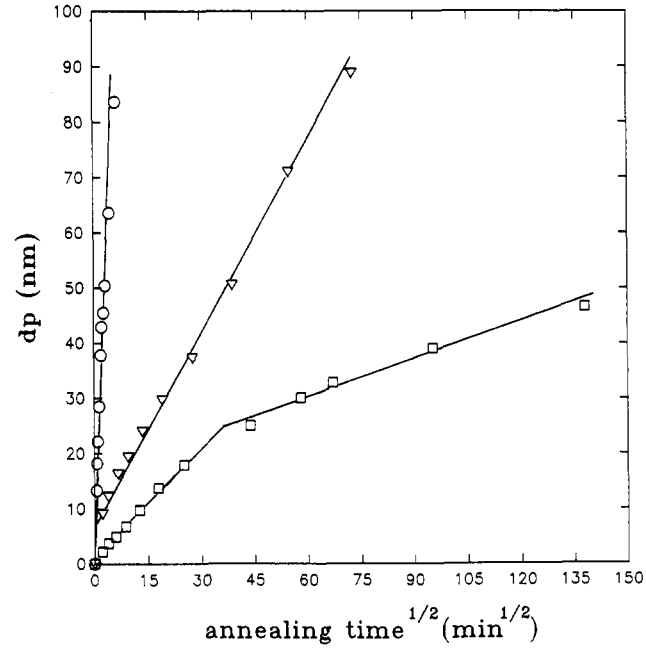

Figure 9. Plots of penetration depth d_p versus the square root of annealing time at 70 °C (□), 90 °C (▽), and 120 °C (○).

differ from 0.35 found for d_p. However no $t^{0.5}$ behavior was found in any of these representations. Figure 8 shows therefore that much attention has to be paid to the definition of the penetration depth within experimental contexts. One should also be aware that only a log–log representation is meaningful to assess the time power law of the penetration depth. This is directly illustrated in Figure 9 which shows the plots of d_p versus the square root of the annealing time at 70, 90, and 120 °C. Linear variations can be observed at all temperatures, although two regimes could also be distinguished at 70 °C. Thus the $t^{0.5}$ behavior of d_p could be inferred with this representation whereas Figure 7 does not support this power law.

Figure 10 shows log–log representations of d_p versus annealing time for films with and without organic solvents, annealed at 70 °C. Two important remarks can be made for films containing solvents: (i) d_p values are larger or

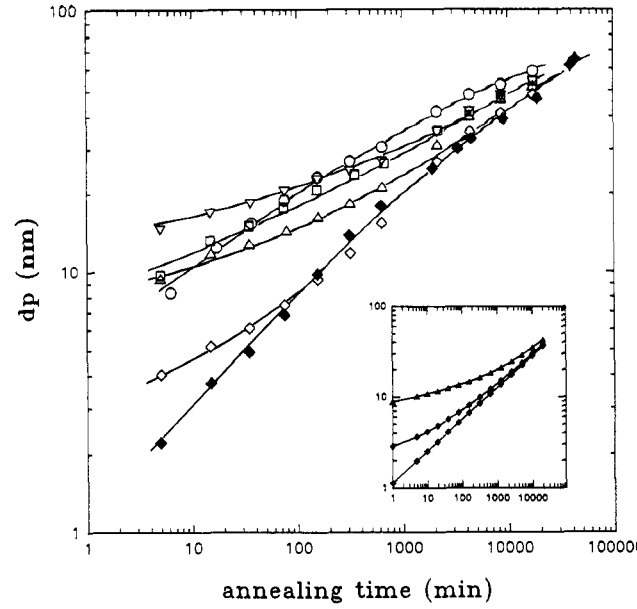

Figure 10. Plots of penetration depth d_p versus annealing time at 70 °C for films containing DA (◇), ABY (△), HG (□), TPM (○), DGB (▽) and no additive (◆). Insert: variation of d_p versus time according to eq 2 with $C = 1.13$ (◆), and eq 3 with $C = 1.13$, $A = 5$, $B = 5$ (◇), and $C = 1.13$, $A = 10$, $B = 1$ (△); $\alpha = 0.35$.

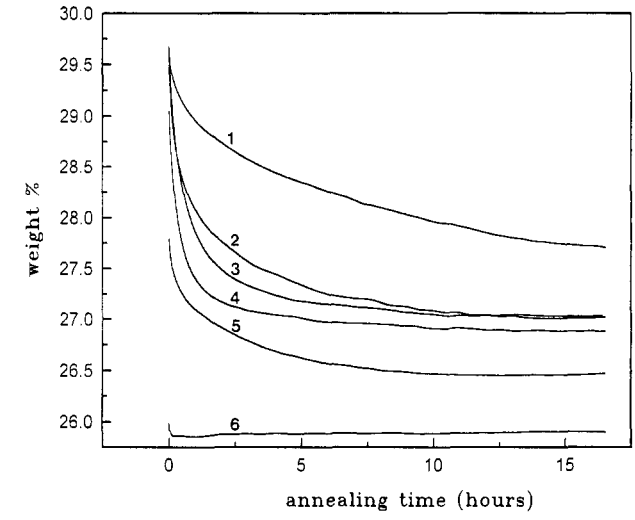

Figure 11. Plots of solvent mass losses versus time at 70 °C for films containing TPM (curve 1), HG (curve 2), DGB (curve 3), ABY (curve 4), DA (curve 5), and no additive (curve 6).

equal to those of an additive-free film. (ii) log–log variations of d_p against t almost exhibit two linear regimes. The three types of behavior distinguished in f_m versus t plots (see Figure 4) can also be observed in Figure 10: (i) The effect of DA is only sensible at early annealing times, below about 2 h. After 2 h of annealing DA is not efficient any longer since the variation of d_p is obviously close to that of the additive-free film. The change of slope after 90 min is quite pronounced and supports the idea that two regimes may be present. (ii) ABY, HG, and DGB show substantial effects on d_p that perdure over long periods of time. Here also d_p plots exhibit remarkable changes of slope, but at longer annealing times than for DA. (iii) TPM presents a one-regime behavior which is totally different from the others. Its d_p values remain the largest at the end of the experiment time (about 2 weeks).

4. Evaporation Rate. The results reported in Figure 6 and 10 can be correlated to the solvent evaporation during annealing. Figure 11 shows plots of the mass losses of the films with and without solvents as a function of annealing time. These results were obtained by TGA as described

in Materials and Methods. After drying at 30 °C for 2 h, almost all the water has been evaporated (see additive-free film curve), so that further observed mass losses could be mainly attributed to solvent evaporation. The percent of mass loss should not exceed 2.6% of the total dispersion since latex dispersions contained 10 wt % based on the polymer of organic solvent. Here again three types of behavior can be distinguished: (i) The DA evaporation rate is the largest. However the total loss is half the one expected, which means that half of DA was evaporated during the drying step at 30 °C. We will also show later that its low plasticizing effect is due to its weak solubility in the polymer. (ii) DGB, HG, and ABY evaporation rates are much lower, which means in practice that their plasticizing effect is more durable than for DA. In fact it appears that the time at which almost the total amount of solvent has evaporated corresponds roughly to the changes of slope on the log–log plots of d_p versus t. (iii) TPM evaporates very slowly: even after 10 000 min (about 7 days), a large amount remained in the film. This result proves that TPM can be more or less considered as a permanent plasticizer.

We have tried to develop a model which describes the variations of d_p with time, introducing a parameter that characterizes the ability of an organic solvent to promote polymer interdiffusion and takes into account the solvent evaporation rate. In the case of an additive-free film, the log–log variation of d_p against time can be considered as linear (see Figure 7). Thus d_p can be expressed by eq 8

$$d_p = Ct^{\alpha} \tag{8}$$

where C represents a function of the diffusion coefficient D and α is the characteristic power law of our polymer system (entangled PBMA chains). Indeed, α was found to be independent of the annealing temperature T and equal to 0.35 ± 0.10, whereas C increases with T and therefore with D (see Figure 7). Thus we believe that C and α are parameters which characterize the local viscosity and the polymer system, respectively.

The case of a film containing a solvent differs from the additive-free film by the factor C, which has now to account for solvent efficiency and its departure from the film. The expression of d_p is then modified in eq 9, where the C in

$$d_p = \left(C + \frac{A}{1 + B\sqrt{t}}\right)t^{\alpha} + d_{p0} \tag{9}$$

eq 8 is now implemented with a term reflecting the solvent evaporation with two time-independent parameters A and B, and d_{p0} is the initial penetration depth. Notice that evaporation was taken inversely proportional to the square root of t because it is Fickian up to at least 100 min of annealing at 70 °C.[24] The insert in Figure 10 shows simulations of variations of d_p versus time, using eq 8 for the additive-free film and eq 9 for films containing DA and ABY, as examples. These simulations match quite well our experimental curves. However no curve fitting was carried out because eq 9 is thought to be only a qualitative model, and by no means a theoretical expression. Nevertheless the close resemblance between simulated and experimental data seems to indicate that our hypotheses are reliable and eq 9 is meaningful.

5. Partition Coefficients and Glass-Transition Temperatures. The partition coefficient K of the organic solvents between water and polymer phases in latex dispersions is also an important parameter. For a matter of comparison, we determined K as defined by Hoy.[22] Thus K is the ratio of the organic solvent concentration C_w in the water phase to its concentration C_p in the polymer. C_ϕ is the ratio of the additive weight in phase ϕ (ϕ stands for w or p) to the weight of phase ϕ. On the other hand T_g values of films can give an idea of the plastifying effect of solvents. K and T_g values are listed in Table 1. Notice that the K value equal to 13 found for HG is very close to the one equal to 16 found by Hoy.[22] However there is no evidence for a correlation between K and T_g values. One reason for this may be that K is a global partition coefficient. In other words C_p takes into account the total quantity of solvent present in the polymer phase, wherever it is located in the bulk or at the surface, whereas T_g measures directly the plasticizing effect of additive in the polymer bulk. Therefore the partition coefficients K' of solvents between water and dodecane were also determined and are listed in Table 1. Notice that for each solvent, K' is larger than K. If we assume that K' stands for the partition coefficient of solvents between water and polymer bulk, then the difference between K' and K can directly be related to the location of solvent in the particle. The larger the ratio K' to K, the larger the porportion of solvent at particle interfaces. On the basis of this assumption one can conclude that DGB, HG, and ABY are preferentially located in a particle shell at the surface. Thus ABY would even be more localized at the particle surface than DGB and HG. This explains its efficiency as a filming aid at early annealing times (see Figure 10) despite the quite high T_g of its film.

Table 1. K, Partition Coefficient of Solvent between Water and Polymer Phases, K', Partition Coefficient of Solvent between Water and Dodecane, T_g, Glass-Transition Temperature of Film (Additive 10 wt %), and τ_{R_G}, Annealing Time Necessary for Polymer Chains To Travel a Distance R_G

solvent[a]	TPM	DGB	HG	ABY	DA	free
K	0.01	3	13	0.22	8	
K'	0.013	9.1	21.7	3.37	10.8	
T_g (±3 deg)	10	13	16	24	26	36
τ_{R_G} (min)	34	10	35	150	600	600

[a] Solvent Chemical Names are Provided in the Materials section.

6. General Remarks. An important issue in latex film formation or in polymer healing is to know what penetration depth value is necessary in order to fully recover the mechanical strength of the polymer film. Concerning this issue, various experiments have been carried out and several theories of self-adhesion or autohesion already exist.[2,25] The major step to achieve the full strength recovery is the formation of entanglements between polymer chains that diffuse across the interface. Recent theories of interface healing and polymer diffusion are based on the reptation model introduced by de Gennes[26] and developed by others.[27-33] They all led to the conclusion that the interface healing time with respect to mechanical strength is equal to the tube renewal time, in fact the time τ_{R_G} for polymer chains to diffuse one radius of gyration R_G. Experimental works are indeed in agreement with these theoretical predictions.[18,19] In spite of the fact that the interpretation of our experimental data of f_m is based on a Fickian model of diffusion and not on a reptation model, an estimate value of τ_{R_G} can be given, since we know the value of the mean radius of gyration R_G of the polymer chains of our latex (16 nm). Therefore τ_{R_G} is directly obtained from Figure 10. Table 1 reports τ_{R_G} values for each film. Assuming that the full strength of the interface is recovered after τ_{R_G}, we are eventually able to classify solvents from the less to the most efficient organic solvents: DA, ABY, HG ~ TPM, DGB. However small quantities of solvent may remain in films after a

period of time τ_{R_G} (see Figure 11) and therefore may retard full strength recovery of films. In that case the evaporation rate would become a preponderant criterium in the choice of a filming aid. Thus it appears that it will be useful to compare in the future the above conclusions with film mechanical strength measurements.

Conclusion

We have shown the effect of organic solvents on latex film formation in terms of polymer diffusion across particle interfaces. Diffusion coefficient D and penetration depth d_p were found to depend on solvent nature, especially at early annealing times, showing large differences with values in additive-free films, but also, and maybe even more strongly, on solvent evaporation rate which appeared to be a critical factor in the role of a filming aid. A model simulating solvent evaporation and taking into account the initial penetration depth, in the behavior of d_p versus annealing time, happened to match quite well with experimental curves. Thus distinctions could be made between solvents, which can simply act as a cosolvent like DA (fast evaporation, poor plasticizer) or a remanent plasticizer like TPM (weak evaporation, strong plasticizer), or a filming aid, i.e. HG, DGB, and ABY (moderate evaporation rate, fairly good plasticizer). Penetration depth d_p values at early annealing times actually give a good indication of the plasticizing effect of solvents, and the total annealing time necessary to retrieve an additive-free film behavior determines the duration of solvent efficiency.

Acknowledgment. The authors thank Elf Aquitaine and Elf Atochem for their financial support of this research and their interest in the project. Mr. Yves Guilbert (ICS Strasbourg) is also gratefully acknowledged for his help in performing thermogravimetric analysis measurements.

References and Notes

(1) Bradford, E. B.; Vanderhoff, J. W. *J. Macromol. Chem.* **1966**, *1*, 335. *J. Macromol. Sci., Phys.* **1972**, *6*, 671. Vanderhoff, J. W.; Bradford, E. B.; Carrington, W. K. *J. Polym. Sci., Polym. Symp.* **1973**, *41*, 155. Padget, J. C.; Moreland, P. J. *J. Coat. Technol.* **1983**, *55*, 39.
(2) Voyutskii, S. S. *J. Polym. Sci.* **1958**, *32*, 528. *Autohesion and Adhesion of High Polymers*; John Wiley & Sons: New York, 1963.
(3) Pekcan, Ö.; Winnik, M. A.; Croucher, M. D. *Macromolecules* **1990**, *23*, 2673.
(4) Zhao, C.-L.; Wang, Y.; Hrushka, Z.; Winnik, M. A. *Macromolecules* **1990**, *23*, 4082.
(5) Wang, Y.; Zhao, C.-L.; Winnik, M. A. *J. Chem. Phys.* **1991**, *95*, 2143.
(6) Wang, Y.; Winnik, M. A. *Macromolecules* **1990**, *23*, 4731.
(7) Winnik, M. A.; Wang, Y.; Haley, F. *J. Coat. Technol.* **1992**, *64* (811), 51.
(8) Juhué, D.; Wang, Y.; Winnik, M. A. *Makromol. Chem., Rapid Commun.* **1993**, *14*, 345.
(9) *Polymer Handbook*, 3rd ed.; John Wiley & Sons: New York, 1989.
(10) Pfeffer, G.; Lami, H.; Laustriat, G.; Coche, A. *C. R. Hebd. Séances Acad. Sci.* **1963**, *257*, 434.
(11) Förster, Th. *Ann. Phys. (Leipzig)* **1948**, *2*, 55. *Discuss. Faraday Soc.* **1959**, *27*, 7.
(12) Walker, K. R. In *Additives for Water-based Coatings*; Karsa, D. R., Ed.; The Royal Society of Chemistry: Cambridge, U.K., 1990.
(13) Carslaw, H. S.; Jaeger, J. C. *Conduction of Heat in Solids*, 1st ed.; Oxford Press: Oxford, U.K., 1959.
(14) Crank, J. *The Mathematics of Diffusion*; Clarendon Press: Oxford, U.K., 1975.
(15) More details on the numerical method will be published elsewhere by Winnik et al.
(16) Hahn, K.; Ley, G.; Schuller, H.; Oberthür, R. *Colloid Polym. Sci.* **1986**, *64*, 1029.
(17) Hahn, K.; Ley, G.; Oberthür, R. *Colloid Polym. Sci.* **1988**, *66*, 631.
(18) Yoo, J. N.; Sperling, L. H.; Glinka, C. J.; Klein, A. *Macromolecules* **1991**, *24*, 2868.
(19) Yoo, J. N.; Sperling, L. H.; Glinka, C. J.; Klein, A. *Macromolecules* **1990**, *23*, 3962.
(20) Linné, M. A.; Klein, A.; Sperling, L. H.; Wignall, G. D. *J. Macromol. Sci., Phys.* **1988**, *B27*, 181. Linné, M. A.; Klein, A.; Miller, G. A.; Sperling, L. H.; Wignall, G. D. *J. Macromol. Sci., Phys.* **1988**, *B27*, 217.
(21) Wang, Y.; Winnik, M. A. Personal communication.
(22) Hoy, K. *J. Paint Technol.* **1973**, *45*, 51.
(23) Wang, Y.; Winnik, M. A. *J. Phys. Chem.* **1993**, *97*, 2507.
(24) Juhué, D. Ph.D. Thesis, Strasbourg (France), in preparation.
(25) Tirrell, M. *Rubber Chem. Technol.* **1984**, *57*, 523.
(26) de Gennes, P. G. *C. R. Séances Acad. Sci. Paris* **1980**, *B291*, 219.
(27) Kim, Y. H.; Wool, R. P. *Macromolecules* **1983**, *16*, 1115.
(28) Prager, S.; Tirrell, M. *J. Chem. Phys.* **1981**, *75*, 5194.
(29) Prager, S.; Adolf, D.; Tirrell, M. *J. Chem. Phys.* **1983**, *78*, 7015.
(30) Adolf, D.; Tirrell, M.; Prager, S. *J. Polym. Sci., Polym. Phys. Ed.* **1985**, *23*, 413.
(31) Prager, S.; Adolf, D.; Tirrell, M. *J. Chem. Phys.* **1986**, *84*, 5152.
(32) Wool, R. P.; O'Connor, K. M. *J. Appl. Phys.* **1981**, *52*, 5194.
(33) Whitlow, S. J.; Wool, R. P. *Macromolecules* **1991**, *24*, 5926.